Cellular/Molecular

Proton-Mediated Block of Ca^{2+} Channels during Multivesicular Release Regulates Short-Term Plasticity at an Auditory Hair Cell Synapse

Soyoun Cho and Henrique von Gersdorff
The Vollum Institute, Oregon Health & Science University, Portland, Oregon 97239

Synaptic vesicles release both neurotransmitter and protons during exocytosis, which may result in a transient acidification of the synaptic cleft that can block Ca^{2+} channels located close to the sites of exocytosis. Evidence for this effect has been reported for retinal ribbon-type synapses, but not for hair cell ribbon synapses. Here, we report evidence for proton release from bullfrog auditory hair cells when they are held at more physiological, *in vivo*–like holding potentials ($V_h = -60$ mV) that facilitate multivesicular release. During paired recordings of hair cells and afferent fibers, L-type voltage-gated Ca^{2+} currents showed a transient block, which was highly correlated with the EPSC amplitude (or the amount of glutamate release). This effect was masked at $V_h = -90$ mV due to the presence of a T-type Ca^{2+} current and blocked by strong pH buffering with HEPES or TABS. Increasing vesicular pH with internal methylamine in hair cells also abolished the transient block. High concentrations of intracellular Ca^{2+} buffer (10 mM BAPTA) greatly reduced exocytosis and abolished the transient block of the Ca^{2+} current. We estimate that this transient block is due to the rapid multivesicular release of ~600–1300 H^+ ions per synaptic ribbon. Finally, during a train of depolarizing pulses, paired pulse plasticity was significantly changed by using 40 mM HEPES in addition to bicarbonate buffer. We propose that this transient block of Ca^{2+} current leads to more efficient exocytosis per Ca^{2+} ion influx and it may contribute to spike adaptation at the auditory nerve.

Key words: **auditory; calcium current; electrophysiology; exocytosis; hair cells; protons**

Introduction

The firing of action potentials causes intracellular and extracellular pH changes at diverse types of neurons and synapses (Ballanyi and Kaila, 1998; Chesler, 2003; Kim and Trussell, 2009). Recently, rapid pH changes have been observed at *Drosophila* nerve terminals during high-frequency *in vivo* activity (Caldwell et al., 2013; Rossano et al., 2013). These changes are mediated by the activation of transporters and pumps in the plasma membrane, but they can also be mediated in part by the exocytosis of protons (H^+) from synaptic vesicles because the lumen of secretory vesicles is estimated to be very acidic (Miesenböck et al., 1998; Einhorn et al., 2012; pH ≅5.5–5.7). This release of vesicular protons can transiently acidify the narrow synaptic cleft and lead to a rapid block of nearby Ca^{2+} channels because low pH shifts the activation curve of Ca^{2+} currents to more depolarized voltages and reduces the peak current amplitude (Barnes et al., 1993; Klöckner and Isenberg, 1994). This occurs because the pores of Ca^{2+} channels contain glutamate residues that can bind H^+ ions at a site close the channel mouth and this extremely fast binding reduces Ca^{2+} channel conductance (Prod'hom et al., 1987, 1989; Chen et al., 1996).

To date, evidence for a block of Ca^{2+} currents by vesicular protons has come primarily from retinal ribbon-type synapses (DeVries, 2001; Palmer et al., 2003; Jarsky et al., 2010). At these synapses, presynaptic L-type Ca^{2+} channels are located a few nanometers from docked synaptic vesicles within specialized active zones that contain a synaptic ribbon organelle (Zenisek et al., 2003; Vaithianathan and Matthews, 2014). However, auditory and vestibular hair cells also contain synaptic ribbons (Liberman et al., 1990; Nouvian et al., 2006). Here, graded membrane potential changes, sometimes fluctuating in the submillisecond time scale and as small as 0.2 mV, are able to gate the entry of Ca^{2+} ions through L-type Ca^{2+} channels (Russell and Sellick, 1983; Spassova et al., 2001). The resulting rapid changes in free Ca^{2+} ion concentration trigger glutamate release at the basal pole of hair cells in response to sound-evoked signals. This rapid secretion of neurotransmitter occurs via a highly synchronous form of multivesicular release (Glowatzki and Fuchs, 2002; Grant et al., 2010; Schnee et al., 2013), although fusion pore flickering of uniquantal release may also play a role (Chapochnikov et al., 2014). Recent studies suggest that protons are also released from vestibular hair cells and may act as nonquantal neurotransmitters that directly affect postsynaptic nerve terminals (Highstein et

Received June 6, 2014; revised Sept. 2, 2014; accepted Sept. 23, 2014.

Author contributions: S.C. and H.v.G. designed research; S.C. performed research; S.C. and H.v.G. analyzed data; S.C. and H.v.G. wrote the paper.

This work was supported by a National Institutes of Health–National Institute on Deafness and Other Communication Disorders Grant DC004274 to H.v.G. and by a Deafness Research Foundation grant to S.C. We thank Evan Vickers and Mean-Hwan Kim for discussions.

The authors declare no competing financial interests.

Correspondence should be addressed to Henrique von Gersdorff, The Vollum Institute, Oregon Health & Science University, Portland, OR 97239; E-mail: vongersd@ohsu.edu.

DOI:10.1523/JNEUROSCI.2304-14.2014

 0270-6474/14/3415877-11$15.00/0

al., 2014). However, evidence for an effect of released protons on Ca^{2+} channels has not been described for hair cell synapses.

Here, we show that a copious amount of protons are released from auditory hair cells in the bullfrog amphibian papilla. We reveal the features that can mask this effect, such as underlying T-type Ca^{2+}currents, hyperpolarized resting membrane potentials, and specific drugs that change vesicle or extracellular pH buffering strength. We also show that multivesicular release promotes synaptic cleft acidification. Finally, we suggest that this proton-mediated Ca^{2+} channel block may function to reduce unnecessary Ca^{2+} influx, increase exocytosis efficiency, and modulate short-term plasticity.

Materials and Methods

Hair cell preparation. After an Oregon Health & Science University Institutional Animal Care and Use Committee–approved animal care protocol, amphibian papillae were carefully dissected from adult female or male bullfrogs (*Rana catesbeiana*) as described by Keen and Hudspeth (2006) and Li et al. (2009). Amphibian papillae were placed in a recording chamber with artificial perilymph containing the following (in mM): 95 NaCl, 2 KCl, 2 $CaCl_2$, 1 $MgCl_2$, 25 $NaHCO_3$, 3 glucose, 1 creatine, and 1 Na-pyruvate with pH adjusted to 7.30 with NaOH and continuously bubbled with 95% O_2 and 5% CO_2 (230 mOsm). The external solution at pH 8.9 contained 10 mM TABS [N-tris(hydroxymethyl)-methyl-4-aminobutanesulfonic acid; pK_a 8.9]. During the recordings, the preparation was continuously perfused (2–3 ml/min) with oxygenated artificial perilymph.

Electrophysiology. Semi-intact preparations of hair cells and their connecting afferent fibers were viewed with an Olympus BX51WI microscope equipped with a 60× water-immersion objective lens (Olympus) and digital CCD camera (QImaging). For whole-cell recordings, patch pipettes of borosilicate glass were pulled to resistances of 5–6 MΩ for hair cells and 7–10 MΩ for afferent fibers. Unless noted otherwise, pipettes were filled with the control intracellular solution containing the following (in mM): 77 Cs-gluconate, 20 CsCl, 1 $MgCl_2$, 10 TEA-Cl, 10 HEPES, 2 EGTA, 3 Mg-ATP, 1 Na-GTP, and 5 Na_2-phosphocreatine adjusted to pH 7.3 with CsOH. For internal solutions containing 10 mM methylamine (CH_3NH_2), a reduced amount of Cs-gluconate was used to match osmolarity (230 mOsm). Whole-cell voltage-clamp recordings were performed with an EPC-10/2 (HEKA) patch-clamp amplifier and Patchmaster software (HEKA) at room temperature. Hair cells were held at a resting membrane potential of either −60 mV or −90 mV and afferent fibers were held at −90 mV. Membrane potentials were corrected for a liquid junction potential of 10 mV. Whole-cell calcium currents were not leak subtracted. The averaged uncompensated series resistances in whole-cell recordings were 10.8 ± 0.2 MΩ for hair cells ($n = 20$) and 23.7 ± 1.7 MΩ for afferent fibers ($n = 18$). Whole-cell recordings were electronically compensated by 0% to 30% depending on the uncompensated series resistance to maintain a constant series resistance throughout the recordings.

Capacitance measurements. The measurements of the whole-cell membrane capacitance (C_m) from hair cells were performed under voltage-clamp conditions with the "Sine + DC" method (Lindau and Neher, 1988; Gillis, 2000) using an EPC-10/2 (HEKA) patch-clamp amplifier and Patchmaster software (HEKA). Patch pipettes were coated with dental wax to minimize their stray capacitance and to achieve better C-fast compensation. Sine waves (50 mV peak-to-peak, 1 or 2 kHz) were superposed on the holding potential, which was set to either −90 mV or −60 mv, and the resulting current response was used to calculate C_m via a Patchmaster software emulator of a lock-in amplifier (Gillis, 2000). The average whole-cell capacitance of hair cells was 11.6 ± 0.3 pF ($n = 20$). The increase of C_m (ΔC_m) evoked by membrane depolarization was measured as $\Delta C_m = C_{m\ (response)} - C_{m\ (baseline)}$ and was used as a measure of synaptic vesicle exocytosis from hair cells. An average of $C_{m\ (response)}$ and $C_{m\ (baseline)}$ was obtained by averaging capacitance data points before and after the depolarizing pulse.

Data analysis. Data analysis was performed with Igor Pro (Wavemetrics) and Prism (GraphPad Software) software. Statistical significance was assessed with paired and unpaired Student's t tests. Data are expressed as mean ± SEM.

Results

Ca^{2+} currents and synaptic transmission at different hair cell holding potentials

We performed paired whole-cell recordings of hair cells and their afferent fibers. The depolarization of hair cells activates Ca^{2+} currents and the subsequent increase in Ca^{2+} ion concentration triggers glutamate release. However, the profile of the Ca^{2+} currents was different depending on the hair cell holding potential (Fig. 1*A*; Cho et al., 2011). When hair cells were depolarized from −60 mV, which is close to the physiological resting membrane potential of hair cells (Crawford and Fettiplace, 1980; Pitchford and Ashmore, 1987), to a potential of −30 mV, the Ca^{2+} currents showed a "notch". This notch was absent in the Ca^{2+} currents of hair cells that were held at −90 mV ($n = 19$; Fig. 1*A*). We called this initial notch in the Ca^{2+} current a "transient block" (Fig. 1*A2*). Hair cells of the frog (*Rana pipiens*) sacculus also exhibit a similar notch in their Ca^{2+} currents, although the details of this notch were not studied (Rutherford and Roberts, 2006). The average size of the transient block was 22.9 ± 2.6% of the peak Ca^{2+} current ($n = 19$). Importantly, the average EPSC peak amplitudes were significantly larger when hair cells were held at a holding potential of −60 mV than when they were held at −90 mV (Fig. 1*A2*,*C*; $n = 11$). Moreover, the initial EPSCs elicited from hair cells held at −60 mV had a fast rise time that reflected the synchronous release of several vesicles because quantal size (single vesicle release) at this synapse has been shown to be ~50–60 pA (Li et al., 2009; Fig. 1*A2*). The resting Ca^{2+} concentration inside hair cells held at −60 mV is probably higher than at −90 mV because some of Ca^{2+} channels are activated and remain open at −60 mV (Graydon et al., 2011). This higher level of resting Ca^{2+} may lead to facilitation of glutamate release and thus to larger EPSCs. This may also contribute to calmodulin-mediated facilitation of Ca^{2+} channel opening kinetics, faster vesicle recruitment, and shorter synaptic delays (Cho et al., 2011; Goutman and Glowatzki, 2011).

Ca^{2+} current kinetics and synaptic delays at different holding potentials

We next investigated how the resting membrane potential of hair cells affects the kinetics of Ca^{2+} current activation and the synaptic delay by holding the same hair cell first at −90 mV and then at −60 mV. The delay time of the Ca^{2+} current onset was determined by the time between the beginning of the depolarizing pulse and the onset of Ca^{2+} currents (Goutman and Glowatzki, 2011). For hair cells held at −60 mV, the delay time of the Ca^{2+} current onset was 0.12 ± 0.03 ms ($n = 6$), which was significantly shorter than that for hair cells held at −90 mV (0.56 ± 0.04 ms, $n = 6$; $p = 0.0002$, paired t test). Next, the synaptic delay was measured from the beginning of the depolarizing pulse to the onset of the EPSC. As expected from the faster Ca^{2+} current kinetics, the synaptic delay became significantly shorter by changing the holding potential of hair cells from −90 mV (1.77 ± 0.18 ms, $n = 6$) to −60 mV (0.99 ± 0.08 ms, $n = 6$; $p = 0.0014$, paired t test). These results are similar to those from rat inner hair cell (IHC) synapses, in which the resting membrane potential of IHCs determines release probability and synaptic delay (Goutman and Glowatzki, 2011; Goutman, 2012). We hypothesized that this facilitated condition of hair cells at −60 mV may affect

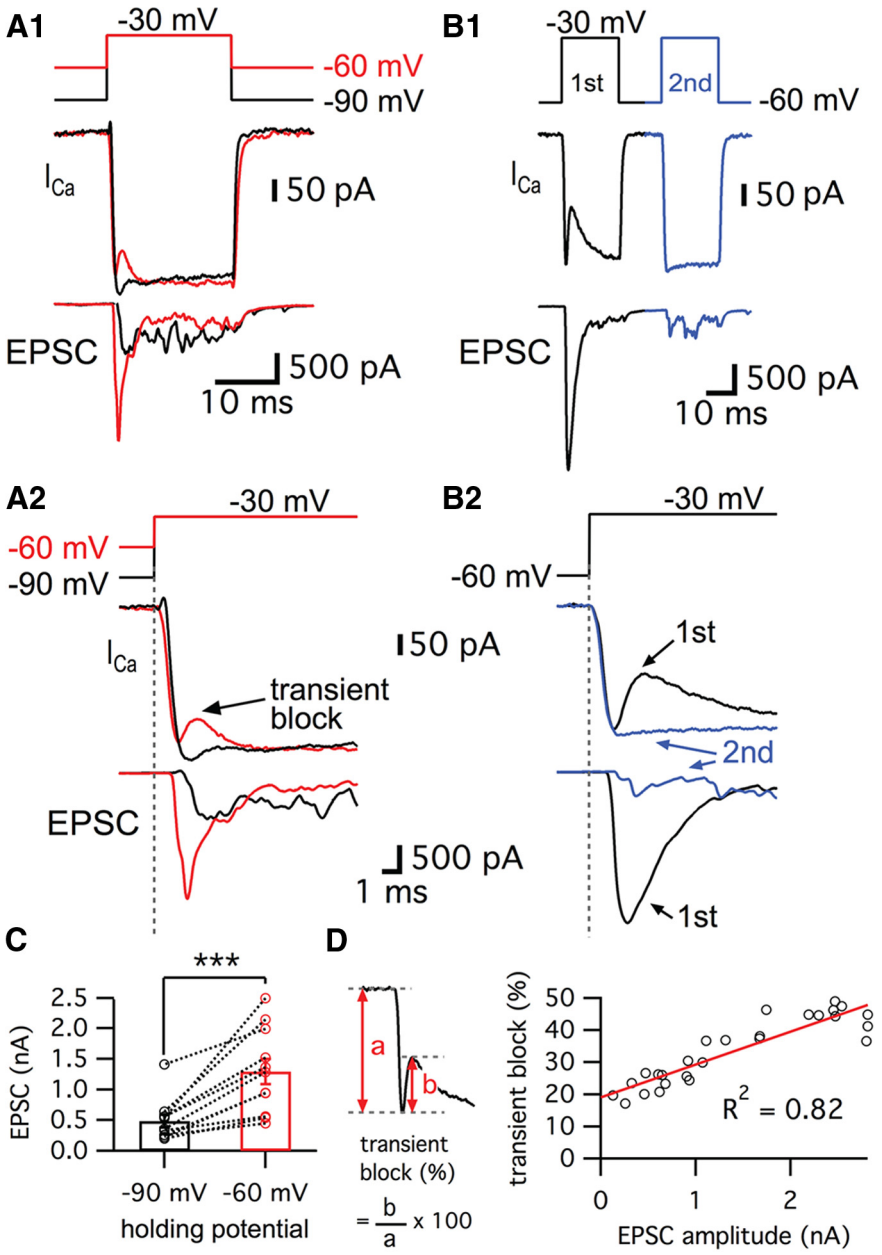

Figure 1. Ca^{2+} currents of bullfrog hair cells exhibit a transient block at a holding potential of −60 mV. ***A***, Paired whole-cell voltage-clamp recordings of presynaptic hair cell and a connected afferent fiber. The hair cell was depolarized from −90 mV (black) or −60 mV (red) to −30 mV for 20 ms (***A1***). When a hair cell was held at −60 mV, the postsynaptic afferent fiber showed a larger EPSC than for hair cells at −90 mV (***A2***). At −60 mV, the Ca^{2+} current showed a transient block in contrast with Ca^{2+} currents of hair cells at −90 mV (***A2***). EPSCs evoked by stimulating hair cells from −60 mV (red) showed shorter synaptic delay than that for hair cells at −90 mV (black) (***A2***). ***B***, When the hair cells were stimulated by a pair of 20 ms pulses from −60 to −30 mV, the transient block was observed in the first Ca^{2+} current (black in ***B1***) with large EPSCs and was absent in the second Ca^{2+} current (blue in ***B1***). With strong paired-pulse depression, the second Ca^{2+} current does not show the transient block. ***B2*** shows overlapped traces of Ca^{2+} currents with EPSCs from ***B1*** on an expanded time scale. ***C***, The peak amplitudes of EPSCs were significantly increased by changing the holding potential of hair cells from −90 mV (485 ± 104 pA) to −60 mV (1292 ± 208 pA) within the same pairs of recordings ($n = 11$, $p < 0.001$, paired t test). Open circles indicate individual pairs. ***D***, The ratio of transient block in Ca^{2+} currents was measured from the amplitude of transient block (b) divided by the peak amplitude of Ca^{2+} currents (a). The ratio of transient block strongly correlates with the amplitude of the EPSCs ($n = 27$ measurements from 7 pairs). The red line shows a linear fit (slope = 0.010 ± 0.001, $R^2 = 0.82$).

the efficiency of release. We estimated the efficiency of release by calculating the ratio of EPSC charge to Ca^{2+} charge transfer during a 20 ms pulse and then changing the membrane holding potential from −90 to −60 mV. The calculated efficiency of release was significantly increased from 0.75 ± 0.17 at −90 mV to 1.62 ± 0.46 at −60 mV ($n = 8$, with $p < 0.05$, paired t test). This suggests that hair cells with a resting membrane potential at −60 mV are in a facilitated mode, with a higher efficiency of release and a transient block of Ca^{2+} current that decreased the Ca^{2+} charge transfer during a 20 ms pulse.

Studies of goldfish retinal bipolar cell terminals reveal that depolarization activates an L-type current and the release of protons that transiently block the Ca^{2+} current, although this effect does not depend on the holding potential (data not shown; Palmer et al., 2003). We thus hypothesized that H^+ ions are released from fused vesicles and transiently block the Ca^{2+} currents of hair cells. This hypothesis is supported by the results with larger EPSC amplitudes from hair cells held at −60 mV (Fig. 1*A*). To confirm whether the transient block of Ca^{2+} currents is tightly correlated with the amount of transmitter release, we stimulated hair cells using a pair of depolarizing pulses (Fig. 1*B*). Hair cell synapses showed strong paired-pulse depression when we held the cells at −60 mV (Cho et al., 2011). This presumably reflects rapid vesicle pool depletion. We observed that, for a large EPSC, the first Ca^{2+} current had a large transient block (Fig. 1*B*). However, the transient block was absent in the second Ca^{2+} current, which elicited very small and asynchronous EPSCs (Fig. 1*B*). This was confirmed over several paired recordings when we plotted the size of the transient block against the EPSC amplitudes (Fig. 1*D*). The size of transient block, measured as the ratio of transient block amplitude divided by the peak amplitude of the Ca^{2+} current, had a linear relationship with the amplitude of the corresponding EPSC (Fig. 1*D*; $n = 27$ measurements from 7 different paired recordings). This strong correlation suggests that the source of the rapid and transient block in the Ca^{2+} current in hair cells may be the fast release of protons via multivesicular exocytosis similar to the situation of retina bipolar cell ribbon synapses (Palmer et al., 2003).

How much time is required for hair cells to be held at −60 mV so that one can begin to detect the transient block of the Ca^{2+} currents? To answer this, we depolarized hair cells from −90 to −60 mV for various durations as a prepulse and then depolarized to −30 mV for 20 ms to elicit a sizable Ca^{2+} current (Fig. 2*A*). Note that the depolarization from −90 to −60 mV also evoked a small and non-inactivating Ca^{2+} current (27.5 ± 7.1 pA, $n = 6$; Fig. 2*A*,*B*). We propose that this tonic Ca^{2+} current plays a pivotal role in facilitating release by establishing an ele-

vated level of resting Ca^{2+} at −60 mV that increases release probability (Cho et al., 2011; Goutman and Glowatzki, 2011). The transient block required ~50–100 ms at −60 mV to start being detectable. Moreover, the size of the transient block increased as hair cells were held longer at −60 mV ($n = 5$; Fig. 2*C*). Interestingly, this time duration required for a detectable transient block (50–100 ms) seems to also be required for complete inactivation of the T-type currents. It may also be a time period required for the facilitation of release (Awatramani et al., 2005).

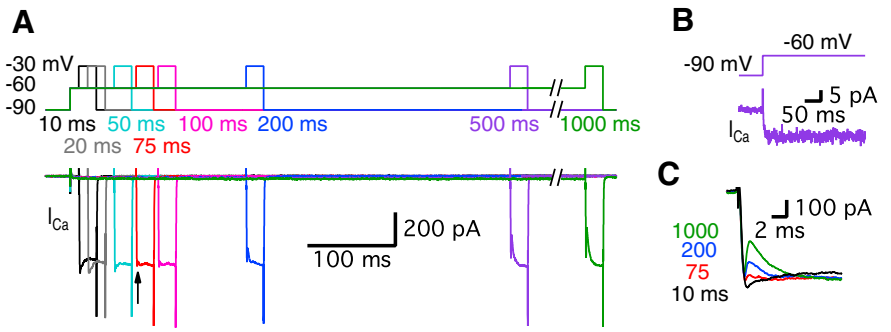

Figure 2. The transient block of the Ca^{2+} current requires a certain period of time at the more depolarized holding potential of −60 mV. ***A***, Ca^{2+} currents were recorded from hair cells held at −90 mV using a 20-ms-long pulse to −30 mV followed by pre-depolarization to −60 mV for 10–1000 ms. Different colors represent different durations of the pre-depolarization from −90 to −60 mV. Ca^{2+} currents started showing a transient block with 75 ms of pre-depolarization (arrow). ***B***, A depolarization from −90 to −60 mV evokes a small, non-inactivating Ca^{2+} current in the hair cell. ***C***, Ca^{2+} currents elicited by the 20 ms pulses with various pre-depolarization (10, 75, 200, and 1000 ms) were superimposed. The transient block becomes clearly larger as the duration of the pre-depolarization increases.

L-type and T-type Ca^{2+} currents are present in amphibian papilla hair cells

Next, we investigated further why hair cells at −90 mV do not show an obvious transient block in their Ca^{2+} currents. Even considering the smaller amount of released vesicles (Fig. 1*C*), we should have seen some small trace of H^+ ions being released from synaptic vesicles. Interestingly, a recent study shows that T-type Ca^{2+} channels as well as L-type contribute to transmitter release in chick auditory hair cells during development (Levic and Dulon, 2012). We investigated whether adult bullfrog auditory hair cells also have this additional type of voltage-gated Ca^{2+} current. When we blocked L-type Ca^{2+} channels using 10 μM isradipine, Ca^{2+} currents of hair cells held at −90 mV were strongly inhibited and we observed an almost complete block of exocytosis ($n = 5$; Fig. 3*A1*). The average peak amplitude of the isradipine-insensitive Ca^{2+} current was 42.9 ± 7.1 pA ($n = 5$) and this current inactivated quickly with a single exponential decay time constant (3.8 ± 0.4 ms; $n = 5$, Fig. 3*A2*). This suggests that the isradipine-insensitive Ca^{2+} current may mask the transient block while hair cells are held at −90 mV. In contrast, 10 μM isradipine completely blocked the Ca^{2+} current for cells held at −60 mV ($n = 5$; Fig. 3*B*), presumably because the T-type current was already inactivated at −60 mV. Based on this activation profile and the fast kinetics of inactivation, the isradipine-insensitive currents are probably T-type Ca^{2+} currents (Hille, 2001). However, T-type Ca^{2+} currents do not appear to significantly contribute to exocytosis because 10 μM isradipine almost completely blocked the changes in membrane capacitance (ΔC_m; $n = 5$) even for a 500 ms long depolarizing pulse. Therefore, as at other auditory hair cell synapses (Spassova et al., 2001; Brandt et al., 2005), L-type Ca^{2+} channels mediate the triggering of transmitter release at adult bullfrog hair cell synapses.

Underlying mechanisms that cause the transient block of the Ca^{2+} current

Our data suggest that the transient block of Ca^{2+} currents results from vesicle release. During exocytosis, vesicles release protons that can inhibit Ca^{2+} channels that are located near the release sites (Fig. 4*A*). To confirm the relationship between transient block of Ca^{2+} currents and the release of synaptic vesicles, we changed the intracellular Ca^{2+} buffers from 2 mM EGTA (our control Ca^{2+} buffer) to 10 mM BAPTA, a higher concentration of a faster Ca^{2+} buffer (Fig. 4*B*). A high concentration of BAPTA is known to make evoked release less synchronous in addition to reducing the amount of release in response to a stimulus (Goutman and Glowatzki, 2007). Indeed, with 10 mM BAPTA, hair cells held at both −60 mV and −90 mV showed greatly reduced ΔC_m (Fig. 4*B*; Graydon et al., 2011). When hair cells are held at −60 mV, the average ΔC_m evoked by a 500 ms pulse in control (2 mM EGTA) was 160.9 ± 14.4 fF ($n = 8$), and this became significantly smaller in 10 mM BAPTA (17.3 ± 3.7 fF, $n = 8$, $p < 0.0001$, unpaired t test). When hair cells are held at −90 mV, the average ΔC_m evoked by a 500 ms pulse in control (2 mM EGTA) was 147.3 ± 9.1 fF ($n = 34$), but ΔC_m decreased to 17.5 ± 2.8 fF with 10 mM BAPTA ($n = 8$, $p < 0.0001$, unpaired t test). With a 500 ms pulse, the efficiency of release of hair cells at −60 mV significantly decreased in 10 mM BAPTA (0.13 ± 0.02 fF/pC, $n = 8$) compared with control (1.55 ± 0.32 fF/pC, $n = 8$; $p = 0.0006$, unpaired t test). When hair cells were held at −90 mV, the efficiency of release evoked by a 500 ms pulse was also significantly decreased in 10 mM BAPTA (0.13 ± 0.03 fF/pC, $n = 8$) compared with control (1.27 ± 0.15 fF/pC, $n = 9$; $p < 0.0001$, unpaired t test). The lack of a "notch" in the Ca^{2+} current for cells held at −60 mV ($n = 9$) confirms that this effect is tightly correlated with the amount of exocytosis. With 10 mM BAPTA, the difference between the Ca^{2+} currents for hair cells held at −60 mV and −90 mV is probably due to T-type Ca^{2+} currents (Fig. 3*A2*). We conclude that the transient block requires the nearly synchronous release of several vesicles, because a small amount of H^+ ions released in an asynchronous manner may simply be quickly buffered within the synaptic cleft before it reaches Ca^{2+} channels. Therefore, the absence of transient block with 10 mM BAPTA suggests that the evoked release of vesicles needs to be copious and highly synchronous in response to a stimulus to overwhelm the local pH buffers within the cleft and thus inhibit Ca^{2+} channels effectively.

Our control internal solutions include 2 mM EGTA as a Ca^{2+} buffer and it is known that Ca^{2+} binding activity of EGTA is sensitive to pH (Tsien, 1980; Naraghi, 1997). To show that the transient block of Ca^{2+} current was not due to the properties of EGTA itself, we confirmed that the transient block of Ca^{2+} currents still existed using 0.5 mM BAPTA, a Ca^{2+} buffer that is much less sensitive to pH changes. Hair cells with 0.5 mM BAPTA exhibited exocytosis via ΔC_m jumps and showed a transient block of Ca^{2+} current ($n = 9$; data not shown). This again suggests that the transient block of Ca^{2+} current is due to the release of H^+ ions.

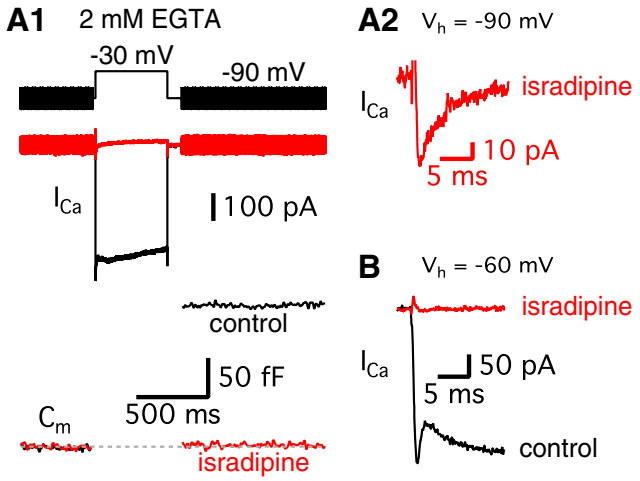

Figure 3. T-type Ca^{2+} currents mask the transient block for hair cells held at −90 mV. ***A1***, A hair cell was depolarized from −90 to −30 mV for 500 ms in control (black) and after perfusion of 10 μM isradipine, a specific L-type Ca^{2+} channel blocker (red). The standard intracellular hair cell Ca^{2+} buffer was 2 mM EGTA. 10 μM isradipine strongly inhibited Ca^{2+} currents and the C_m jump elicited by the depolarizing pulse. ***A2***, After applying isradipine, a small Ca^{2+} current still persists in hair cells held at −90 mV (red). ***B***, After holding hair cells at −60 mV, isradipine completely blocked the Ca^{2+} current (red).

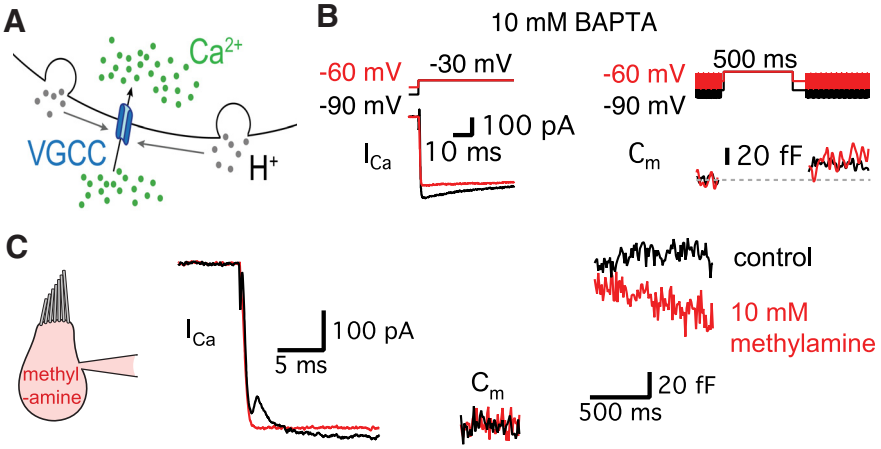

Figure 4. The transient block of Ca^{2+} current requires the exocytosis of synaptic vesicles. ***A***, Diagram showing that H^+ (gray) ions are released from fused vesicles during exocytosis and can affect adjacent Ca^{2+} channels at an active zone of release (blue). ***B***, After the dialysis of 10 mM BAPTA into a hair cell, Ca^{2+} currents were evoked by a 500 ms pulse from −90 mV (black) or from −60 mV (red) to −30 mV. Note that Ca^{2+} currents do not show the transient block now that exocytosis has been severely decreased by 10 mM BAPTA. ***C***, 10 mM methylamine was added to the internal pipette solution. This removed the transient block, which went from 81 ± 15 to 0 pA ($n = 6$, $p = 0.0028$, paired t test) without significant changes in ΔC_m (136 ± 2.4 fF in control and 126 ± 4.8 fF in 10 mM methylamine, $n = 6$, $p > 0.05$, paired t test). The Ca^{2+} current was evoked by a 500-ms-long pulse from a holding potential of −60 to −30 mV. The Ca^{2+} currents were recorded in control (black) with a first patch pipette and then, after repatching the same hair cell, using a second pipette containing 10 mM methylamine (red).

Another way to confirm that vesicular protons cause the transient block is to dialyze 10 mM methylamine (CH_3NH_2), a weak base, into the hair cells via the patch pipette. Methylamine can remove the vesicular pH gradient (Johnson, 1987; Cousin and Nicholls, 1997). Indeed, in goldfish bipolar cells, 10 mM methylamine removed the transient block in Ca^{2+} currents without affecting exocytosis or reciprocal GABAergic feedback (Vigh et al., 2005). When we applied methylamine to hair cells, the transient block was removed without altering vesicle release measured by ΔC_m ($n = 6$; Fig. 4*C*). This directly suggests that the transient block results from the exocytosis of vesicular protons that inhibit Ca^{2+} currents. Apparently, with methylamine, hair cells still release vesicles normally, but they cannot release free protons that transiently acidify the cleft.

In mouse bipolar cells, a chloride-selective glutamate transporter current can cause a "notch" in the presynaptic Ca^{2+} current (Snellman et al., 2011). To determine whether glutamate transporters contribute to the "notch" of Ca^{2+} currents in hair cells, we blocked the transporters using 100 μM DL-*threo*-β-benzyloxyaspartic acid (TBOA). However, hair cells still showed the transient block of Ca^{2+} current with TBOA and the duration of pre-depolarization to −60 mV needed for the transient block to become apparent was similar to that of control (Fig. 5*A*; $n = 6$; see also Fig. 2*C*; data not shown). The transient block of Ca^{2+} current was thus unaffected by the presence of TBOA. Therefore, glutamate transporters do not contribute to the transient block of hair cell Ca^{2+} currents.

A previous study with amphibian papillae hair cells of leopard frogs suggested that the transient block in the Ca^{2+} current was due to a slowly activating and rapidly inactivating K^+ current (I_K) because it remained after 10 mM TEA but was removed by 1 mM 4-aminopyridine (4-AP; Smotherman and Narins, 1999). 4-AP is a membrane-permeable K^+ current blocker (Armstrong and Loboda, 2001) and is also used clinically in the treatment of multiple sclerosis because it enhances transmitter release (Fujihara and Miyoshi, 1998). When we applied 1 or 10 mM 4-AP to the external bath, the transient block of the Ca^{2+} current was also removed ($n = 15$; Fig. 5*B*,*C*). This confirms the previous results. When we applied 10 mM 4-AP via the patch pipette solution, it also significantly decreased the amplitude of transient block ($n = 9$; $p = 0.0011$, paired t test; Fig. 5*D*) without changing ΔC_m (27.9 ± 3.0 fF in control and 28.1 ± 3.1 fF in 4-AP; $n = 9$; $p > 0.05$, paired t test). However, application of external 20 mM TEA with a Cs^+-based intracellular patch pipette solution still could not affect the "notch" of the Ca^{2+} current, suggesting that it was not due to an I_K current ($n = 5$; data not shown). Moreover, the transient inhibition was more prominent at $V_h = -60$ mV (Fig. 1), a potential at which a putative inactivating I_K should be less prominent. Together, these seemingly contradictory results suggest that the blocking effect of 4-AP on the "notch" of Ca^{2+} current was not due to its block of voltage-gated K^+ currents. Instead, we propose that the effect of 4-AP is through its H^+-capturing ability as a weak base similar to methylamine. Indeed, it has been shown that 4-AP can work as a weak base that quickly crosses the plasma membrane (Guse et al., 1994; Gobet et al., 1995).

Remarkably, a very similar "notch" in the Ca^{2+} current of catfish electroreceptors, which also form ribbon-type synapses, has been reported previously (Sugawara, 1989). This "notch" was blocked by 4-AP and was strongly correlated to transmitter release with paired recordings of the afferent fibers (Sugawara and Obara, 1989). Given the above results, we suggest that fish elec-

troreceptors may also release protons that produce a transient block of their Ca^{2+} currents.

Changes in extracellular pH buffer strength

We also attempted to change the transient block by changing the extracellular pH buffer. When the strength of external pH buffering was increased by adding 40 mM HEPES in addition to the control $NaHCO_3$, the amplitude of the transient block was significantly decreased from 69.8 ± 13.6 to 0.8 ± 0.8 pA ($n = 10$, $p = 0.0007$, paired t test) without significantly changing ΔC_m (131.4 ± 11.3 fF in control and 129.4 ± 12.0 fF in 40 mM HEPES, $n = 8$, $p > 0.05$, paired t test; Fig. 6*A*; $n = 15$). With 40 mM HEPES, protons are thus normally released from fused vesicles as in control conditions. However, this high concentration of HEPES in the synaptic cleft can quickly capture protons before they reach the Ca^{2+} channels. This result supports the hypothesis that H^+ ions released from synaptic vesicles cause the transient block of Ca^{2+} currents.

We next lowered the extracellular proton concentration with a high-pH buffer (Fig. 6*B*). Previous studies have shown that alkaline pH solutions shift the Ca^{2+} channel activation IV curve to the left and increase the peak inward currents (Barnes et al., 1993; Zhou and Jones, 1996; Palmer et al., 2003). Indeed, with a TABS-based external solution at pH 8.9, we observed both a significantly larger Ca^{2+} current amplitude (48 ± 8% increase, $n = 6$) and ΔC_m (60 ± 20% increase, $n = 6$) evoked by a step depolarization from −60 to −30 mV ($n = 6$; Fig. 6*B1*,*B3*). This greatly enhanced ΔC_m should have increased the transient block of the Ca^{2+} current. Nevertheless, the transient block of Ca^{2+} current quickly disappeared within 2–3 min, the time course of our external bath perfusion system (Fig. 6*B2*). We thus propose that even though the amount of exocytosis was enhanced by larger Ca^{2+} influx, building a strong buffering environment within the synaptic cleft that quickly mops up the released H^+ ions can severely interfere with the transient block of the Ca^{2+} current. These results also indicate that presynaptic Ca^{2+} current amplitude can be tonically controlled by the external pH (Schnee and Ricci, 2003; Fahrenfort et al., 2009).

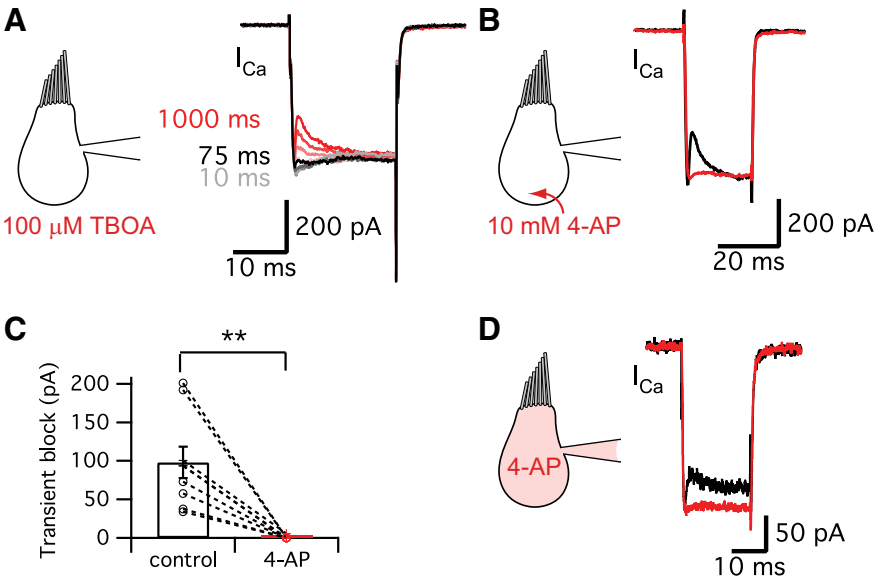

Figure 5. Glutamate transporter and K^+ currents do not contribute to the transient block. ***A***, Ca^{2+} currents were evoked in hair cells held at −90 mV using a pre-depolarization to −60 mV for 10–1000 ms and then by a 20-ms-long pulse to −30 mV (same protocol as Fig. 2*A*). The Ca^{2+} currents for the 20 ms pulses are shown superimposed. The transient block of the Ca^{2+} currents was not blocked by 100 µM TBOA, a specific blocker of glutamate transporters ($n = 6$). The different colors represent different durations of the pre-depolarization. The Ca^{2+} current started showing the transient block within ~75 ms of the pre-depolarization, which was very similar to control (Fig. 2*C*). ***B***, 4-AP removed the transient block of the Ca^{2+} current. However, this effect may not be related with the blocking of K^+ currents, but rather is probably due to the H^+ capturing ability of 4-AP and its possible disruption of normal vesicle pH. ***C***, 10 mM 4-AP significantly decreased the amplitude of transient block from 98 ± 20 pA to 0.6 ± 0.6 pA ($n = 9$). **$p < 0.01$, paired t test. Open circles indicate individual pairs. ***D***, When hair cells were depolarized from −60 to −30 mV for 20 ms, 10 mM 4-AP in the patch pipette solution significantly decreased the transient block from 52.0 ± 9.4 pA (black) to 2.2 ± 2.1 pA (red, $n = 9$, $p = 0.0011$, paired t test). Control recordings were performed within 27 ± 7 s ($n = 9$) after break-in and the recordings of 4-AP effects were done at 4 min 39 ± 30 s ($n = 9$) after break-in to whole-cell mode.

Short-term plasticity and the transient block of Ca^{2+} currents

To determine the physiological role of the transient block, we next changed our stimulating protocol into a train of stimulation at the characteristic frequency of our hair cells, which are electrically tuned to ~400 Hz (Li et al., 2009). When we stimulated hair cells held at −60 mV with a 400 Hz train of 1 ms pulses, the Ca^{2+} currents showed a transient block initially and the corresponding EPSCs were strongly depressed (Fig. 7*A*, black traces). The averaged peak Ca^{2+} currents of hair cells during the train had a double-exponential time course with fast ($\tau_{fast} = 3.9$ ms; 86%) and slow ($\tau_{slow} = 23.7$ ms) time constants ($n = 6$; Fig. 7*A*). The averaged evoked EPSCs were quickly depressed during the train of stimuli ($\tau_{fast} = 1.3$ ms with 91% and $\tau_{slow} = 7.4$ ms; Fig. 7*A*). Enhancing the extracellular pH buffer strength by adding 40 mM HEPES removed the transient block of the Ca^{2+} currents and the depression of the corresponding EPSC trains became slower (Fig. 7*A*, red; $\tau = 2.6$ ms). When we compare the normalized individual EPSCs from the same pair of recordings before (control; Fig. 7*B*, black) and after adding 40 mM HEPES (Fig. 7*B*, red), the second EPSC in the control showed significantly stronger depression than the 40 mM HEPES condition. The averaged ratio of the first and the second EPSCs ($EPSC_2/EPSC_1$) was significantly increased from 0.28 ± 0.03 ($n = 6$) to 0.42 ± 0.04 ($n = 6$) after 40 mM HEPES removed the transient block of Ca^{2+} currents ($p < 0.01$, paired t test; Fig. 7*C*). The average τ of the EPSC train depression became significantly slower with 40 mM HEPES (from 1.4 ± 0.2 to 2.6 ± 0.3 ms; $n = 6$; $p < 0.05$, paired t test; Fig. 7*D*).

We also studied the effect of 4-AP on the transient block during a 400 Hz train of stimuli identical to that of Figure 7*A*. Perfusion with an external solution containing 10 mM 4-AP removed the transient block and slowed the EPSC train depression (Fig. 7*E*). The average paired-pulse ratio of the first two EPSCs was significantly enhanced by 4-AP (from 0.28 ± 0.05 to 0.45 ± 0.06; $n = 5$; $p < 0.01$, paired t test; Fig. 7*F*). The average τ of the EPSC peaks was also significantly increased from 1.8 ± 0.2 to 3.5 ± 0.6 ms by 10 mM 4-AP ($n = 5$; $p < 0.05$, paired t test; Fig. 7*G*). These results are very similar to the effects of 40 mM HEPES (Fig. 7*A*). Interestingly, the time course of this rapid and pronounced depression matches well that of the fast spike rate adaptation of some *in vivo* auditory nerve fiber recordings from bullfrog amphibian papilla (Megela and Capranica, 1982). Importantly, *in vivo* fibers tuned to 400–500 Hz showed the fastest and

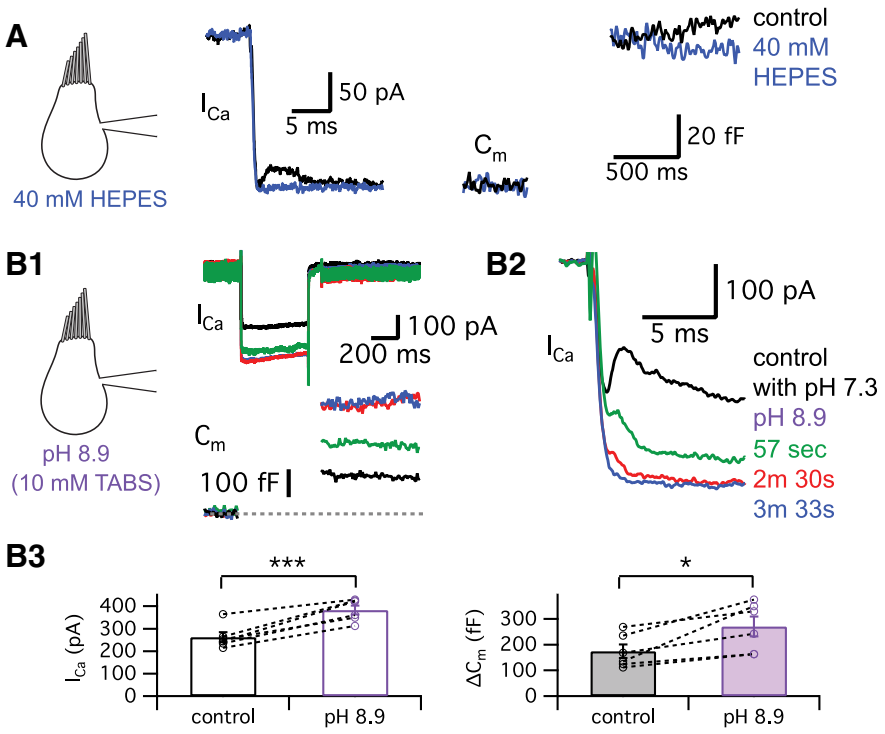

Figure 6. Protons released during exocytosis cause a transient block of Ca^{2+} currents. ***A***, The hair cell was depolarized from −60 to −30 mV for 500 ms in control condition (black) and after perfusion of external solution including 40 mM HEPES (blue). ***B***, External solution of pH 8.9 with 10 mM TABS increased the amplitude of Ca^{2+} currents and the ΔC_m jump, but inhibited the transient block of Ca^{2+} currents. Initial kinetics of the Ca^{2+} currents in ***B1*** are shown in an expanded time scale in ***B2***. As a pH 8.9 solution was applied, the transient block of Ca^{2+} currents was quickly removed. The time lapsed after a control recording as the pH 8.9 solution was being perfused is shown in different colors. In ***B3***, we quantify the effects of the external solution with pH 8.9. The amplitudes of Ca^{2+} currents (left) and ΔC_m (right) evoked by a 500-ms-long depolarization from −60 to −30 mV are compared in control (black) and after >3–5 min of perfusion with the pH 8.9 solution (purple). The average amplitude of Ca^{2+} currents was significantly increased from 262 ± 22 to 383 ± 20 pA ($n = 6$) and ΔC_m was significantly enhanced from 174 ± 26 to 271 ± 39 fF ($n = 6$) by pH 8.9 external solution. *$p < 0.05$, paired t test; ***$p = 0.001$, paired t test. Open circles indicate individual pairs.

strongest adaptation (Megela, 1984). We thus propose that the transient block of the Ca^{2+} currents, together with rapid vesicle pool depletion, may contribute to the fast adaptation of frog auditory nerve responses by reducing Ca^{2+} influx and transmitter release.

Discussion

Our results show that the proton-mediated transient block of Ca^{2+} current decreases Ca^{2+} influx and transmitter release during a high-frequency stimulus train. This inhibitory effect of released protons on Ca^{2+} currents was only apparent when hair cells exhibit enhanced and synchronous multivesicular release. Moreover, this form of release was facilitated when hair cells were held at more depolarized and physiological membrane potentials such as −60 mV. The synaptic delay was also shorter compared with those of hair cells held at −90 mV (Figure 1). Figure 2*B* shows that depolarization of hair cells from −90 to −60 mV evokes a small, non-inactivating Ca^{2+} current. This may elevate the resting Ca^{2+} concentration of hair cells. Release probability will thus be higher and synaptic vesicles may be more primed for release in hair cells held at −60 mV. The transient block is thus much weaker at −90 mV because less release occurs and this release is more asynchronous (Figure 1). In addition, the activation of a T-type Ca^{2+} current masks the transient block when hair cells are held at −90 mV (Fig. 3). Although auditory hair cell Ca^{2} currents do exhibit a Ca^{2+}-dependent inactivation, this has a slow (seconds) time course (Schnee and Ricci, 2003; Graydon et al., 2011).

Comparisons with other ribbon and conventional synapses

Given the tight coupling of Ca^{2+} channels to docked vesicles at many synapses, one must ask, why has the proton-mediated block of Ca^{2+} channels not been observed at more synapses and particularly at conventional active zone synapses? Detectable transient block will be determined by many factors, such as the kinetics of voltage-gated Ca^{2+} channels, the distance between release sites and Ca^{2+} channels, the amount and the synchronicity of exocytosis, and the structure of the synaptic cleft. L-type Ca^{2+} channels are located under or adjacent to synaptic ribbons (Rutherford and Pangršič, 2012). Moreover, a distinctive feature of ribbon synapses is the occurrence of multiple docked vesicles that can be released within a very short period of time onto a narrow synaptic cleft (20 nm wide). This compact ultrastructure makes ribbon synapses especially susceptible to the transient acidification by H^+ ions released from multiple vesicles and optimizes the conditions for observing a transient block of the Ca^{2+} channels. In contrast, the calyx of Held synapse has ~500 conventional active zones distributed over a large presynaptic area. The release probability is low and heterogeneous and Ca^{2+} channels are also located at some distance from docked vesicles at immature synapses (Wang et al., 2008; Leão and von Gersdorff, 2009), so the transient block is not seen, although the overall EPSC is synchronous and quite large (up to 20 nA). Recently, proton release was observed to trigger *C. elegans* muscle contraction (Beg et al., 2008) and synaptic cleft acidification has been observed with imaging techniques at photoreceptor ribbon synapses (Wang et al., 2014) and at conventional synapses of the amygdala (Du et al., 2014). Finally, we note that electroreceptors display many similarities to auditory hair cells and, surprisingly, also display a "notch" in their Ca^{2+} current (Sugawara, 1989).

Why has the transient block of Ca^{2+} current not been seen at mammalian inner hair cell synapses? We suggest several explanations. First, the pH buffer used in the external solutions will certainly play a key role. We routinely use bicarbonate, a physiological buffer. Second, the transient block was only detectable when we held hair cells at −60 mV (Fig. 1). This facilitated release and inactivated the T-type current that masks the transient block (Fig. 3; Levic and Dulon, 2012). We thus suggest that the transient block is observed more clearly under more depolarized and *in vivo*–like hair cell holding potentials. Third, using 4-AP to block K^+ channels also prevents the transient block because 4-AP can function as a weak base that may alter cytosol or vesicle pH (Guse et al., 1994; Gobet et

al., 1995). Fourth, the amount of carbonic anhydrase in the synaptic cleft may be an important factor. Strong expression of carbonic anhydrase has been found in mammalian cochlea and this fast enzyme may prevent the transient block (Ichimiya et al., 1994; Okamura et al., 1996). Fifth, the small size of afferent fiber terminals in mammals (~2–3 μm) may prevent the transient block by allowing the rapid escape of released protons from the synaptic cleft.

How many protons in a single synaptic vesicle?

A possible role for the proton gradient between the vesicular lumen and the synaptic cleft may be to accelerate the rapid release of glutamate (Brown et al., 2010). Recent studies show that the time constant of vesicle acidification is fast (τ = 0.5–1 s in Budzinski et al., 2011, and τ = 5 s at 25°C in Granseth and Lagnado, 2008). It is thus possible that the concentration of H^+ contained within vesicles of hair cells changes rapidly with changes in membrane potential. However, this seems unlikely for our hair cells because the time period for the transient block to become manifest was extremely fast (only 50–100 ms; Fig. 2*C*).

How many protons can be released from a fused vesicle? To estimate this, we use the mean vesicle inner diameter of 32.9 nm (Graydon et al., 2011). This gives the volume of a single vesicle: 2×10^{-20} L. Assuming the concentration of glutamate in vesicles as 100–200 mM (Naito and Ueda, 1985; Burger et al., 1989), a single vesicle contains ~1200–2400 glutamate molecules. Synaptic vesicular pH is estimated to vary from 5.3 to 5.7 at conventional synapses (Miesenböck et al., 1998; Sankaranarayanan et al., 2000) and may vary from 5.0 to 6.5 at hair cells (Einhorn et al., 2012; Neef et al., 2014). Here, we assume a vesicle pH of 5.5 (DeVries, 2001) and estimate that the number of free H^+ in a vesicle is <1. Consider that pH is defined as the logarithm of the reciprocal of H^+ activity ($pH = -\log_{10} a_{H+}$). The activity of H^+ (a_{H+})is a product of the concentration of H^+ ($[H^+]$) and activity coefficient (g), which depends on temperature and the ionic strength of the solution ($a_{H+} = g \cdot [H^+]$; Covington et al., 1985; Fujishiro et al., 1994). Assuming that g is 1 to simplify our calculation, $[H^+]$ in a vesicle with pH 5.5 is $10^{-5.5}$ M (3.16×10^{-6} M). Considering the volume of a single vesicle (2×10^{-20} L) and Avogadro's constant (6.022×10^{23} mol^{-1}), a single vesicle contains ~0.04 free H^+. Even if we assume that g is 0.1, there are 0.4 free H^+ per single vesicle. However, the number of bound protons within vesicles may be much larger because synaptic vesicles contain 1200–2400 glutamate molecules and the pK_a of glutamate is 4.1. The Henderson-Hasselbalch equation states:

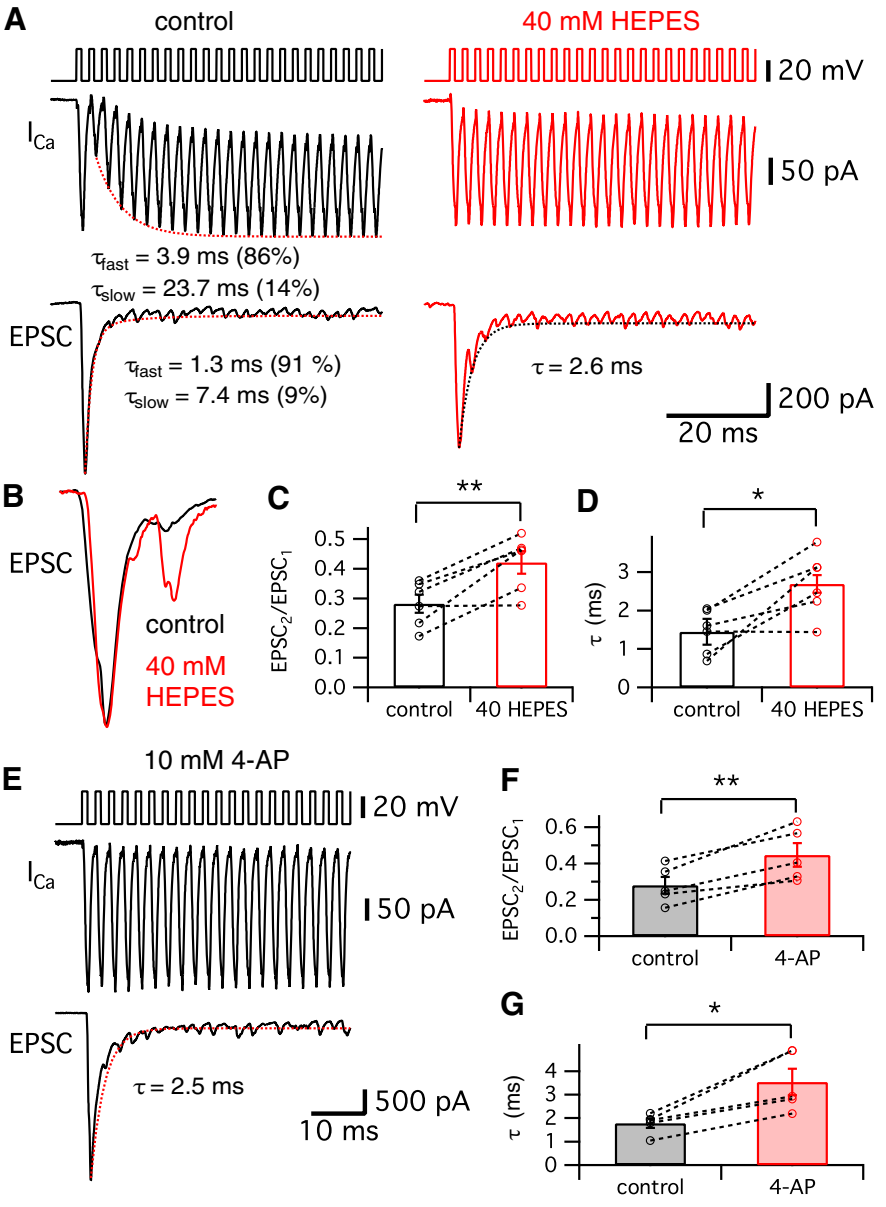

Figure 7. Effects of released H^+ ions on EPSC amplitudes during a 400 Hz train of stimuli. ***A***, Hair cells were stimulated by a train of 1 ms depolarizing pulses from −60 to −30 mV with an interpulse interval of 1.5 ms. A total of 40 stimuli were given at 400 Hz for 100 ms. Ca^{2+} currents showed a transient block with a double exponential recovery (dashed line; τ_{fast} = 3.9 ms and τ_{slow} = 23.7 ms) in control (left). EPSCs evoked by the 400 Hz train of pulses showed depression (dashed line; τ_{fast} = 1.3 ms and τ_{slow} = 7.4 ms). After perfusion of the external solution with added 40 mM HEPES (right), the hair cell Ca^{2+} currents do not show the transient block and the corresponding EPSCs show depression with a single exponential time constant (τ = 2.6 ms). ***B***, EPSCs in control (black) and 40 mM HEPES (red) were normalized and superimposed. The second and third EPSCs become larger when 40 mM HEPES removed the transient block in the Ca^{2+} currents. Note that the second EPSC (arrow) was significantly larger with 40 mM HEPES than in control. ***C***, The ratio of the first and the second EPSCs ($EPSC_2/EPSC_1$) in control (black) and with 40 mM HEPES (red). $EPSC_2/EPSC_1$ with 40 mM HEPES was significantly increased (0.42 ± 0.04) compared with that in control (0.28 ± 0.03; n = 6). ***D***, From 6 pairs, the average τ of the EPSC peaks in 40 mM HEPES (red, 2.6 ± 0.3 ms) was significantly increased compared with control (black, 1.4 ± 0.2 ms). ***E***, When hair cells were stimulated by a 400 Hz train of 1 ms depolarizing pulses from −60 to −30 mV, an external solution with 10 mM 4-AP removed the transient block in Ca^{2+} currents and slowed the kinetics of the EPSC train depression (fit with a single exponential time constant: τ = 2.5 ms). ***F***, $EPSC_2/EPSC_1$ in control (black) and with 10 mM 4-AP (red). $EPSC_2/EPSC_1$ with 10 mM 4-AP was significantly increased (0.45 ± 0.06) compared with that in control (0.28 ± 0.05; n = 5). ***G***, From 5 pairs, the average τ of the EPSC peaks in 10 mM 4-AP (red, 3.5 ± 0.6 ms) was significantly increased compared with control (black, 1.8 ± 0.2 ms). *p < 0.05, paired t test; **p < 0.01, paired t test. Open circles indicate individual pairs.

$$pH = pKa + \log\left(\frac{[A^-]}{[HA]}\right)$$

So the ratio of the negatively charged form of glutamate ($[A^-]$) to glutamic acid ($[HA]$) inside a vesicle is ~25 (for 1200–2400 glutamate molecules, we get 1154–2308 glutamates and 46–92 glutamic acids). After the vesicle fuses with the plasma membrane, this ratio will change to 1585 because the pH in the synaptic cleft is 7.3. This indicates that, after vesicles fuse, all of the glutamate molecules become negatively charged. According to this calculation, ~46–92 glutamic acid molecules release H^+ ions and become deprotonated glutamates per vesicle. How many protons are released during a 20 ms depolarizing pulse? The average ΔC_m evoked by a 20 ms pulse from a holding potential of −60 to −30 mV was 24.2 ± 3.4 fF ($n = 14$). Considering that the membrane capacitance of a single synaptic vesicle is 34 aF, ~700 vesicles are released by a 20 ms pulse and these vesicles release ~32,000–63,000 H^+ ions into the synaptic cleft during a 20 ms pulse. This corresponds to 640–1260 H^+ ions per synaptic ribbon and 16–31 H^+ ions per Ca^{2+} channel (40 Ca^{2+} channels per ribbon and 50 ribbons per hair cell; Graydon et al., 2011). Therefore, because glutamate itself can function as a potent H^+ buffer, the number of bound H^+ ions is much larger than that of free H^+ ions in synaptic vesicles. We thus propose that the combined acidification stemming from multiple vesicles released within a millisecond can transiently overwhelm the pH buffers within the narrow synaptic cleft.

Protons released from fused vesicles also can affect postsynaptic receptors in the afferent fibers. It has been reported that H^+ ions inhibit AMPA receptor activity by enhancing desensitization (Traynelis and Cull-Candy, 1991; Lei et al., 2001). However, ribbon-type synapses, including our bullfrog hair cell synapses, do not appear to exhibit tonic desensitization of AMPA receptors (Singer and Diamond, 2006; Pang et al., 2008; Cho et al., 2011; Graydon et al., 2014). In summary, we propose that the transient block in Ca^{2+} current functions as a negative feedback mechanism that reduces subsequent transmitter release, leads to more efficient exocytosis per Ca^{2+} ion influx, and may also contribute to fast spike rate adaptation in the auditory nerve during sound stimulation (Megela, 1984).

References

Armstrong CM, Loboda A (2001) A model for 4-Aminopyridine action on K channels: Similarities to tetraethylammonium ion action. Biophys J 81:895–904. CrossRef Medline

Awatramani GB, Price GD, Trussell LO (2005) Modulation of transmitter release by presynaptic resting potential and background calcium levels. Neuron 48:109–121. CrossRef Medline

Ballanyi K, Kaila K (1998) Activity-evoked changes in intracellular pH. In: pH and Brain Function (Kaila K, Ransom BR, eds), pp 291–308. New York: Wiley.

Barnes S, Merchant V, Mahmud F (1993) Modulation of transmission gain by protons at the photoreceptor output synapse. Proc Natl Acad Sci U S A 90:10081–10085. CrossRef Medline

Beg AA, Ernstrom GG, Nix P, Davis MW, Jorgensen EM (2008) Protons act as a transmitter for muscle contraction in C. elegans. Cell 132:149–160. CrossRef Medline

Brandt A, Khimich D, Moser T (2005) Few $Ca_V1.3$ channels regulate the exocytosis of a synaptic vesicle at the hair cell ribbon synapse. J Neurosci 25:11577–11585. CrossRef Medline

Brown JT, Weatherall KL, Corria LR, Chater TE, Isaac JT, Marrion NV (2010) Vesicular release of glutamate utilizes the proton gradient between the vesicle and synaptic cleft. Front Synaptic Neurosci 2:15. CrossRef Medline

Budzinski KL, Zeigler M, Fujimoto BS, Bajjalieh SM, Chiu DT (2011) Measurements of the acidification kinetics of single synaptopHluorin vesicles. Biophys J 101:1580–1589. CrossRef Medline

Burger PM, Mehl E, Cameron PL, Maycox PR, Baumert M, Lottspeich F, De Camilli P, Jahn R (1989) Synaptic vesicles immunoisolated from rat cerebral cortex contain high levels of glutamate. Neuron 3:715–720. CrossRef Medline

Caldwell L, Harries P, Sydlik S, Schwiening CJ (2013) Presynaptic pH and vesicle fusion in *Drosophila* larvae neurones. Synapse 67:729–740. CrossRef Medline

Chapochnikov NM, Takago H, Huang C, Pangršič T, Khimich D, Neef J, Auge E, Göttfert F, Hell SW, Wichmann C, Wolf F, Moser T (2014) Uniquantal release through a dynamic fusion pore is a candidate mechanism of hair cell exocytosis. Neuron 83:1389–1403. CrossRef Medline

Chen XH, Bezprozvanny I, Tsien RW (1996) Molecular basis of proton block of L-type Ca^{2+} channels. J Gen Physiol 108:363–374. CrossRef Medline

Chesler M (2003) Regulation and modulation of pH in the brain. Physiol Rev 83:1183–1221. CrossRef Medline

Cho S, Li GL, von Gersdorff H (2011) Recovery from short-term depression and facilitation is ultrafast and Ca2+ dependent at auditory hair cell synapses. J Neurosci 31:5682–5692. CrossRef Medline

Cousin MA, Nicholls DG (1997) Synaptic vesicle recycling in cultured cerebellar granule cells: role of vesicle acidification and refilling. J Neurochem 69:1927–1935. CrossRef Medline

Covington AK, Bates RG, Durst RA (1985) Definition of pH scales, standard reference values, measurement of pH and related terminology. Pure Applied Chemistry 57:531–542.

Crawford AC, Fettiplace R (1980) The frequency selectivity of auditory nerve fibers and hair cells in the cochlea of the turtle. J Physiol 306:79–125. Medline

DeVries SH (2001) Exocytosed protons feedback to suppress the Ca^{2+} current in mammalian cone photoreceptors. Neuron 32:1107–1117. CrossRef Medline

Du J, Reznikov LR, Price MP, Zha XM, Lu Y, Moninger TO, Wemmie JA, Welsh MJ (2014) Protons are a neurotransmitter that regulates synaptic plasticity in the lateral amygdala. Proc Natl Acad Sci U S A 111:8961–8966. CrossRef Medline

Einhorn Z, Trapani JG, Liu Q, Nicolson T (2012) Rabconnectin3α promotes stable activity of the H^+ pump on synaptic vesicles in hair cells. J Neurosci 32:11144–11156. CrossRef Medline

Fahrenfort I, Steijaert M, Sjoerdsma T, Vickers E, Ripps H, van Asselt J, Endeman D, Klooster J, Numan R, ten Eikelder H, von Gersdorff H, Kamermans M (2009) Hemichannel-mediated and pH-based feedback from horizontal cells to cones in the vertebrate retina. PLoS One 4:e6090. CrossRef Medline

Fujihara K, Miyoshi T (1998) The effects of 4-aminopyridine on motor evoked potentials in multiple sclerosis. J Neurol Sci 159:102–106. CrossRef Medline

Fujishiro N, Hatae J, Kawata H (1994) A program for calculation of the proton activity coefficient. Comput Biol Med 24:221–228. CrossRef Medline

Gillis KD (2000) Admittance-based measurement of membrane capacitance using the EPC-9 patch-clamp amplifier. Pflugers Arch 439:655–664. CrossRef Medline

Glowatzki E, Fuchs PA (2002) Transmitter release at the hair cell ribbon synapse. Nat Neurosci 5:147–154. CrossRef Medline

Gobet I, Lippai M, Tomkowiak M, Durocher Y, Leclerc C, Moreau M, Guerrier P (1995) 4-aminopyridine acts as a weak base and a Ca^{2+} mobilizing agent in triggering oocyte meiosis reinitiation and activation in the Japanese clam *Ruditapes philippinarum*. Int J Dev Biol 39:485–491. Medline

Goutman JD (2012) Transmitter release from cochlear hair cells is phase locked to cyclic stimuli of different intensities and frequencies. J Neurosci 32:17025–17035a. CrossRef Medline

Goutman JD, Glowatzki E (2007) Time course and calcium dependence of transmitter release at a single ribbon synapse. Proc Natl Acad Sci U S A 104:16341–16346. CrossRef Medline

Goutman JD, Glowatzki E (2011) Short-term facilitation modulates size and timing of the synaptic response at the inner hair cell ribbon synapse. J Neurosci 31:7974–7981. CrossRef Medline

Granseth B, Lagnado L (2008) The role of endocytosis in regulating the

strength of hippocampal synapses. J Physiol 586:5969–5982. CrossRef Medline

Grant L, Yi E, Glowatzki E (2010) Two modes of release shape the postsynaptic response at the inner hair cell ribbon synapse. J Neurosci 30:4210–4220. CrossRef Medline

Graydon CW, Cho S, Li GL, Kachar B, von Gersdorff H (2011) Sharp Ca^{2+} nanodomains beneath the ribbon promote highly synchronous multivesicular release at hair cell synapses. J Neurosci 31:16637–16650. CrossRef Medline

Graydon CW, Cho S, Diamond JS, Kachar B, von Gersdorff H, Grimes WN (2014) Specialized postsynaptic morphology enhances neurotransmitter dilution and high-frequency signaling at an auditory synapse. J Neurosci 34:8358–8372. CrossRef Medline

Guse AH, Roth E, Emmrich F (1994) Ca^{2+} release and Ca^{2+} entry induced by rapid cytosolic alkalinization in Jurkat T-lymphocytes. Biochem J 301:83–88. Medline

Highstein SM, Holstein GR, Mann MA, Rabbitt RD (2014) Evidence that protons act as neurotransmitters at vestibular hair cell-calyx afferent synapses. Proc Natl Acad Sci U S A 111:5421–5426. CrossRef Medline

Hille B (2001) Voltage-gated calcium channels. In: Ionic channels of excitable membranes, 3rd ed., pp 95–130. Sunderland, MA: Sinauer.

Ichimiya I, Adams JC, Kimura RS (1994) Immunolocalization of Na^+, K^+-ATPase, Ca^{++}-ATPase, calcium-binding proteins, and carbonic anhydrase in the guinea pig inner ear. Acta Otolaryngol 114:167–176. CrossRef Medline

Jarsky T, Tian M, Singer JH (2010) Nanodomain control of exocytosis is responsible for the signaling capability of a retinal ribbon synapse. J Neurosci 30:11885–11895. CrossRef Medline

Johnson RG Jr (1987) Proton pumps and chemiosmotic coupling as a generalized mechanism for neurotransmitter and hormone transport. Ann N Y Acad Sci 493:162–177. CrossRef Medline

Keen EC, Hudspeth AJ (2006) Transfer characteristics of the hair cell's afferent synapse. Proc Natl Acad Sci U S A 103:5537–5542. CrossRef Medline

Kim Y, Trussell LO (2009) Negative shift in the glycine reversal potential mediated by a Ca^{2+}- and pH-dependent mechanisms in interneurons. J Neurosci 29:11495–11510. CrossRef Medline

Klöckner U, Isenberg G (1994) Intracellular pH modulates the availability of vascular L-type Ca^{2+} channels. J Gen Physiol 103:647–663. CrossRef Medline

Leão RM, von Gersdorff H (2009) Synaptic vesicle pool size, release probability and synaptic depression are sensitive to Ca^{2+} buffering capacity in the developing rat calyx of Held. Braz J Med Biol Res 42:94–104. CrossRef Medline

Lei S, Orser BA, Thatcher GR, Reynolds JN, MacDonald JF (2001) Positive allosteric modulators of AMPA receptors reduce proton-induced receptor desensitization in rat hippocampal neurons. J Neurophysiol 85:2030–2038. Medline

Levic S, Dulon D (2012) The temporal characteristics of Ca^{2+} entry through L-type and T-type Ca^{2+} channels shape exocytosis efficiency in chick auditory hair cells during development. J Neurophysiol 108:3116–3123. CrossRef Medline

Li GL, Keen E, Andor-Ardó D, Hudspeth AJ, von Gersdorff H (2009) The unitary event underlying multiquantal EPSCs at a hair cell's ribbon synapse. J Neurosci 29:7558–7568. CrossRef Medline

Liberman MC, Dodds LW, Pierce S (1990) Afferent and efferent innervation of the cat cochlea: quantitative analysis with light and electron microscopy. J Comp Neurol 301:443–460. CrossRef Medline

Lindau M, Neher E (1988) Patch-clamp techniques for time-resolved capacitance measurements in single cells. Pflugers Arch 411:137–146. CrossRef Medline

Megela AL (1984) Diversity of adaptation patterns in responses of eighth nerve fibers in the bullfrog, *Rana catesbeiana.* J Acoust Soc Am 75:1155–1162. CrossRef Medline

Megela AL, Capranica RR (1982) Differential patterns of physiological masking in the anuran auditory nerve. J Acoust Soc Am 71:641–645. CrossRef Medline

Miesenböck G, De Angelis DA, Rothman JE (1998) Visualizing secretion and synaptic transmission with pH-sensitive green fluorescent proteins. Nature 394:192–195. CrossRef Medline

Naito S, Ueda T (1985) Characterization of glutamate uptake into synaptic vesicles. J Neurochem 44:99–109. CrossRef Medline

Naraghi M (1997) T-jump study of calcium binding kinetics of calcium chelators. Cell Calcium 22:255–268. CrossRef Medline

Neef J, Jung S, Wong AB, Reuter K, Pangrsic T, Chakrabarti R, Kügler S, Lenz C, Nouvian R, Boumil RM, Frankel WN, Wichmann C, Moser T (2014) Modes and regulation of endocytic membrane retrieval in mouse auditory hair cells. J Neurosci 34:705–716. CrossRef Medline

Nouvian R, Beutner D, Parsons TD, Moser T (2006) Structure and function of the hair cell ribbon synapse. J Membr Biol 209:153–165. CrossRef Medline

Okamura HO, Sugai N, Suzuki K, Ohtani I (1996) Enzyme-histochemical localization of carbonic anhydrase in the inner ear of the guinea pig and several improvements of the technique. Histochem Cell Biol 106:425–430. CrossRef Medline

Palmer MJ, Hull C, Vigh J, von Gersdorff H (2003) Synaptic cleft acidification and modulation of short-term depression by exocytosed protons in retinal bipolar cells. J Neurosci 23:11332–11341. Medline

Pang JJ, Gao F, Barrow A, Jacoby RA, Wu SM (2008) How do tonic glutamatergic synapses evade receptor desensitization? J Physiol 586:2889–2902. CrossRef Medline

Pitchford S, Ashmore JF (1987) An electrical resonance in hair cells of the amphibian papilla of the frog *Rana temporaria.* Hear Res 27:75–83. CrossRef Medline

Prod'hom B, Pietrobon D, Hess P (1987) Direct measurement of proton transfer rates to a group controlling the dihydropyridine-sensitive Ca^{2+} channel. Nature 329:243–246. CrossRef Medline

Prod'hom B, Pietrobon D, Hess P (1989) Interactions of protons with single open L-type calcium channels: location of protonation site and dependence of proton-induced current fluctuations on concentration and species of permeant ion. J Gen Physiol 94:23–42. CrossRef Medline

Rossano AJ, Chouhan AK, Macleod GT (2013) Genetically encoded pH-indicators reveal activity-dependent cytosolic acidification of *Drosophila* motor nerve terminal in vivo. J Physiol 591:1691–1706. CrossRef Medline

Russell IJ, Sellick PM (1983) Low-frequency characteristics of intracellularly recorded receptor potentials in guinea-pig cochlear hair cells. J Physiol 338:179–206. Medline

Rutherford MA, Pangršič T (2012) Molecular anatomy and physiology of exocytosis in sensory hair cells. Cell Calcium 52:327–337. CrossRef Medline

Rutherford MA, Roberts WM (2006) Frequency selectivity of synaptic exocytosis in frog saccular hair cells. Proc Natl Acad Sci U S A 103:2898–2903. CrossRef Medline

Sankaranarayanan S, De Angelis D, Rothman JE, Ryan TA (2000) The use of pHluorins for optical measurements of presynaptic activity. Biophys J 79:2199–2208. CrossRef Medline

Schnee ME, Ricci AJ (2003) Biophysical and pharmacological characterization of voltage-gated calcium currents in turtle auditory hair cells. J Physiol 549:697–717. CrossRef Medline

Schnee ME, Castellano-Muñoz M, Ricci AJ (2013) Response properties from turtle auditory hair cell afferent fibers suggest spike generation is driven by synchronized release both between and within synapses. J Neurophysiol 110:204–220. CrossRef Medline

Singer JH, Diamond JS (2006) Vesicle depletion and synaptic depression at a mammalian ribbon synapse. J Neurophysiol 95:3191–3198. CrossRef Medline

Smotherman MS, Narins PM (1999) The electrical properties of auditory hair cells in the frog amphibian papilla. J Neurosci 19:5275–5292. Medline

Snellman J, Mehta B, Babai N, Bartoletti TM, Akmentin W, Francis A, Matthews G, Thoreson W, Zenisek D (2011) Acute destruction of the synaptic ribbon reveals a role for the ribbon in vesicle priming. Nat Neurosci 14:1135–1141. CrossRef Medline

Spassova M, Eisen MD, Saunders JC, Parsons TD (2001) Chick cochlear hair cell exocytosis mediated by dihydropyridine-sensitive calcium channels. J Physiol 535:689–696. CrossRef Medline

Sugawara Y (1989) Two Ca current components of the receptor current in the electroreceptors of the marine catfish *Plotosus.* J Gen Physiol 93:365–380. CrossRef Medline

Sugawara Y, Obara S (1989) Receptor Ca current and Ca-gated K current in tonic electroreceptors of the marine catfish *Plotosus.* J Gen Physiol 93:343–364. CrossRef Medline

Traynelis SF, Cull-Candy SG (1991) Pharmacological properties and H^+ sensitivity of excitatory amino acid receptor channels in rat cerebellar granule neurons. J Physiol 433:727–763. Medline

Tsien RY (1980) New calcium indicators and buffers with high selectivity against magnesium and protons: design, synthesis, and properties of prototype structures. Biochemistry 19:2396–2404. CrossRef Medline

Vaithianathan T, Matthews G (2014) Visualizing synaptic vesicle turnover and pool refilling driven by calcium nanodomains at presynaptic active zones of ribbon synapses. Proc Natl Acad Sci U S A 111:8655–8660. CrossRef Medline

Vigh J, Li GL, Hull C, von Gersdorff H (2005) Long-term plasticity mediated by mGluR1 at a retinal reciprocal synapse. Neuron 46:469–482. CrossRef Medline

Wang LY, Neher E, Taschenberger H (2008) Synaptic vesicles in mature calyx of Held synapses sense higher nanodomain calcium concentrations during action potential-evoked glutamate release. J Neurosci 28:14450–14458. CrossRef Medline

Wang TM, Holzhausen LC, Kramer RH (2014) Imaging an optogenetic pH sensor reveals that protons mediate lateral inhibition in the retina. Nat Neurosci 17:262–268. CrossRef Medline

Zenisek D, Davila V, Wan L, Almers W (2003) Imaging calcium entry sites and ribbon structures in two presynaptic cells. J Neurosci 23:2538–2548. Medline

Zhou W, Jones SW (1996) The effects of external pH on calcium channel currents in bullfrog sympathetic neurons. Biophys J 70:1326–1334. CrossRef Medline